

# FABRICATION OF MEMS-BASED ELECTROTHERMAL MICROACTUATORS WITH ADDITIVE MANUFACTURING TECHNOLOGIES

## IZDELAVA ELEKTROTHERMIČNIH AKTUATORJEV NA OSNOVI MIKRO-ELEKTRONSKO-MEHANSKIH SISTEMOV, IZDELANIH Z DODAJNIMI TEHNOLOGIJAMI

Ishak Ertugrul<sup>1,2\*</sup>, Nihat Akkus<sup>2</sup>, Huseyin Yuces<sup>2</sup>

<sup>1</sup>Mus Alparslan University, Faculty of Engineering and Architecture, Department of Computer Engineering, 49250 Mus, Turkey  
<sup>2</sup>Marmara University Faculty of Technology, Department of Mechatronics Engineering, Goztepe Campus, 34722 Kadikoy – Istanbul, Turkey

*Prejem rokopisa – received: 2019-01-30; sprejem za objavo – accepted for publication: 2019-03-27*

doi:10.17222/mit.2019.027

This study aimed to fabricate a bidirectional electrothermal microactuator that can be produced with the conventional micro-electromechanical system (MEMS) fabrication technique, using two-photon polymerization (2PP) and projection micro-stereolithography (PμSL) methods and to compare these methods with each other. The electrothermal microactuator that can move in two directions was designed in accordance with determined criteria. Although the same design was used for the 2PP and PμSL methods, the supporting structures were not produced with the PμSL method. For the PμSL method, the actuator was produced by removing the supports from the original design. Although 2-μm-diameter supports could be fabricated with the 2PP method, it was not possible to produce them with the PμSL method. Furthermore, the 2PP method was found to be better than the PμSL for the production of complex, non-symmetric support structures.

Keywords: MEMS, 2PP, PμSL, thermal actuator, 3D-printer

Avtorji opisujejo študijo izdelave dvosmernega elektrotermičnega aktuatorja s konvencionalno MEMS tehnologijo (angl.: Micro-Electro-Mechanical System), dvofotonsko polimerizacijo (2PP) in metodami projekcijske mikro-stereolitografije (PμSL) in nato primerjavo med njimi. Elektrotermični aktuator, ki se lahko giblje v dveh smereh, so oblikovali v skladu z vnaprej določenimi kriteriji. Čeprav so tako pri metodi 2PP, kot pri metodi PμSL uporabili enak dizajn, podporne strukture niso izdelali z metodo PμSL. Pri metodi PμSL so aktuator izdelali tako, da so odstranili podpore iz originalnega dizajna. Čeprav se lahko podpore premera 2 μm izdelajo z metodo 2PP, le-teh z njo ni bilo možno izdelati. Nadalje avtorji ugotavljajo, da je za izdelavo kompleksnejših nesimetričnih podpornih struktur metoda 2PP primernejša od metode PμSL.

Gljučne besede: MEMS, 2PP, PμSL, termični aktuator, 3D-printer

## 1 INTRODUCTION

It is known that the MEMS fabrication techniques are highly complex and expensive. The demand for MEMS is increasing with the advancement of technology. Therefore, some facilitating and low-cost production techniques are needed.

There are many processing steps and clean-room requirements for the fabrication of traditional MEMS devices. With the development of 3D micro-additive manufacturing technologies, the production costs and processing steps of MEMS devices have been gradually reduced. According to these advancements, it is possible to produce MEMSs in atmospheric air without the need for many operations (e.g., photolithography) and clean rooms. Additionally, challenging production procedures, such as Lithografie-Galvanformung-Abformung (LIGA), used for some materials, are not needed due to 3D micro-additive manufacturing techniques.

Many companies have used the 2PP method with 3D devices. In particular, the Photonic Professional GT and Photonic Professional GT2 products of Nanoscribe have used the 2PP technique very well. It has been seen that nano-size production is possible with these devices.<sup>1</sup> MEMS devices produced with the 2PP method can be used as micro-fluids,<sup>2</sup> micro-mechanical systems,<sup>3-5</sup> optical systems,<sup>6,7</sup> cell structures,<sup>8</sup> and biomedical devices.<sup>9,10</sup> The PμSL method is also used by many companies today. The NanoArch™ is a 3D micro-fabrication equipment based on the PμSL technology. Studies that have been performed with the PμSL method include micro-sensors,<sup>11,12</sup> micro-fluids,<sup>13</sup> optical systems,<sup>14,15</sup> biomedical devices,<sup>16</sup> and mobile phones.<sup>17,18</sup>

General trends show that many MEMS devices that can be produced with conventional MEMS fabrication techniques can also be manufactured with 3D printers. Moreover, it is evident that 3D-printer methods are more advantageous than traditional MEMS methods regarding the process steps and costs.

In this study, the 2PP and PμSL methods, which are 3D MEMS manufacturing techniques, were examined in

\*Corresponding author's e-mail:  
i.ertugrul@alparslan.edu.tr

detail, and an electrothermal microactuator was fabricated with these methods. These two methods were compared with regard to the fabrication results. It is thought that this study will contribute to the literature in terms of fabricating a microdevice through the use and comparison of different methods.

## 2 MATERIALS AND METHODS

### 2.1 Bidirectional electrothermal actuator design

#### 2.1.1 Working principle

The actuator in our study is defined as the U-type. Such actuators are generally composed of both thin and thick arms and have different designs. A U-type actuator is shown in **Figure 1**. In such actuators, voltage is applied to the pads and the thin arm expands due to warming. This event is based on the temperature differences between the thin and thick arms. There is a decrease in the electrical resistance due to the increase in the cross-sectional area of the thick arm. This situation causes a decrease in Joule heating. Due to warming, the expansion occurs in the thin arm. Thus, the thin arm is longer. The actuator’s movement occurs for these reasons.<sup>19</sup>

The bidirectional MEMS-based electrothermal microactuator is designed to move in two directions, right and left. In order for the actuator to move to the right of this design, DC-1 voltage must be applied as shown in **Figure 2**. Thus, if the voltage is connected to the pad attached to the hot arm while the ground is connected to the pad attached to the flexure arm, the actuator moves to the right. If the actuator is expected to move to the left, DC-2 voltage should be applied as shown in **Figure 2**. Since our design is symmetrical and the actuator is incapable of moving to the right and left simultaneously, voltages DC-1 and DC-2 are not applied at the same time. The actuator will move to the right or left according to the user request.

#### 2.1.2 Design conditions

The lengths of the arm and flexure are of great importance for the actuator to move to the right and left. Our design was made in accordance with the following criteria:<sup>19,20</sup>

- The flexure arm must be as thin as possible.

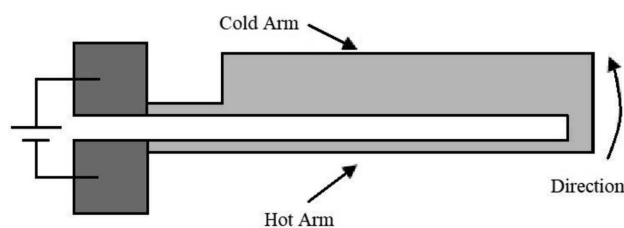


**Figure 1:** U-type actuator<sup>19</sup>

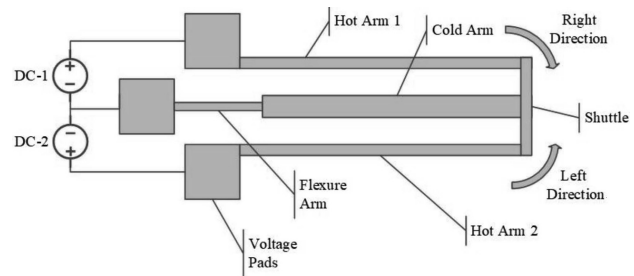


**Figure 2:** Working principle of a bidirectional electrothermal microactuator

- The flexure arm must not be thinner than the hot arms as the flexure arm can overheat and cause deformation.
- The flexure must be long enough to allow the actuator to change directions.
- The flexure must be long enough not to deform the actuator.

As our actuator has a symmetrical structure, dimensioning and designing were performed for a single arm as shown in **Figure 3**.

All the dimensions of our actuator are given in **Table 1**. These values were obtained with the measurements of the actuator made with the 2PP and PμSL methods. The same design was used for both methods. However, since the supporting structures cannot be produced with the PμSL method, the measurements related to the support are given in Section 3.

**Table 1:** Actuator parameters

Parameter	Symbol	Value	Unit
Hot-arm length	$L_h$	250	$\mu\text{m}$
Cold-arm length	$L_c$	200	$\mu\text{m}$
Flexure-arm length	$L_f$	100	$\mu\text{m}$
Actuator gap	$L_g$	7.5	$\mu\text{m}$
Hot-arm width	$w_h$	3	$\mu\text{m}$
Cold-arm width	$w_c$	6	$\mu\text{m}$
Flexure-arm width	$w_f$	3	$\mu\text{m}$
Air-gap thickness	$t_a$	4	$\mu\text{m}$
Actuator thickness	$t$	3	$\mu\text{m}$

### 2.2 2PP technology

The 2PP method has been a widely-used technology in the production of 3D microstructures in recent years. The simplicity and quickness of the fabrication, the pro-

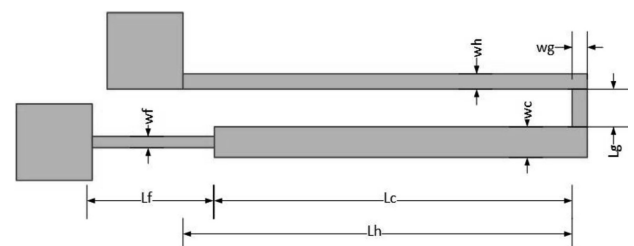


**Figure 3:** Bidirectional electrothermal microactuator dimensions

duction of complex structures, and the high resolution allow this technology to be preferred over the others. Photopolymer materials are used with this method.<sup>21</sup>

In order to fabricate an actuator with the 2PP method, a femtosecond (fs) pulsed laser light source is required. The working principle of 3D microfabrication using the 2PP method is shown in **Figure 4**. Near-infrared (NIR) fs pulses produced with a titanium (Ti) sapphire laser are transformed into visible ones with an optical parametric oscillator (OPO). In order to adjust the intensity of the beam, the light source must enter a neutral density filter (ND). The beam focuses on the sample to initiate polymerization. The photosensitive resin is compacted between two coverslips and mounted on a 3D piezoelectric scanning layer. The motion of the scanning layer is pre-programmed with a computer to generate different microstructures. To analyze the fabrication process, it is recorded with a charge-coupled-device (CCD) camera.<sup>22</sup>

For the 2PP method, the material used in this study was the IP-S resin. **Table 2** gives the properties of this material.

**Table 2:** Material properties of the actuator fabricated with the 2PP method<sup>23,24</sup>

Parameter	Symbol	Value	Unit
Density	$D$	1.2	$\text{g/cm}^3$
Young's modulus	$E$	4.6	GPa
Poisson's ratio	$\nu$	0.35	-
Thermal conductivity	$k_p$	1.82	W/m.K
Thermal expansion coefficient	$\alpha$	0.98	$\mu\text{m/m.K}$
Specific heat capacity	$C$	29	J/kg.K
Electrical resistivity	$R$	2.9	$\mu.\Omega.\text{m}$
Refractive index	$N$	1.48	-

### 2.3 PμSL technology

PμSL is a versatile and cost-effective process that can be used to rapidly generate microlenses, microgrippers, microfluidics and microbeams with electrolysis or resin additives. Materials such as a curable photopolymer, polymer and nanoparticle composites are used with this

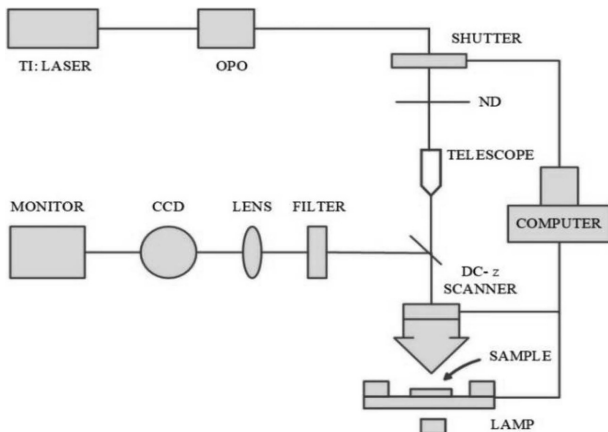


**Figure 4:** Working principle of 3D microfabrication with the 2PP method<sup>22</sup>

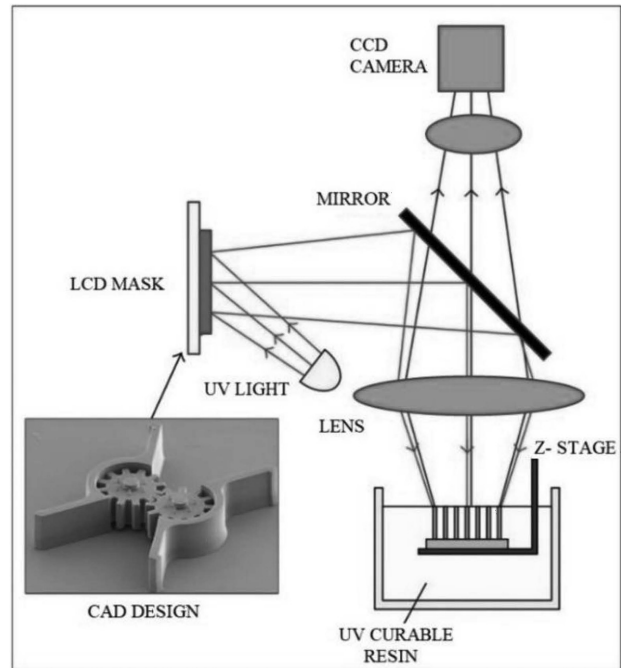


**Figure 5:** Schematic of the working principle of PμSL<sup>25</sup>

method. This method starts by creating a 3D structure using computer-based design (CAD) software and then turns the structure into a set of mask images (digital mask). The working principle of PμSL is shown in **Figure 5**. Each image represents a thin layer of the 3D structure. During a production cycle, a single image is displayed on the reflective liquid crystal display (LCD) panel. The image from the LCD is then reflected on the liquid surface. The whole layer (usually 5–30 μm thick) is polymerized. Once the layer has been solidified, it is re-immersed in the resin to allow a new thin layer of liquid to form. Repeating the loop creates a 3D microstructure from a layer stack.<sup>25</sup>

The properties of the photosensitive resin, which were specially developed for this printer and used in the fabrication of the actuator, are given in **Table 3**.

**Table 3:** Material properties of the actuator fabricated with the PμSL method<sup>26</sup>

Parameter	Symbol	Value	Unit
Density	$D$	0.89	$\text{g/cm}^3$
Young's modulus	$E$	0.9	GPa
Poisson's ratio	$\nu$	0.89	-
Thermal conductivity	$k_p$	1.12	W/m.K
Thermal expansion coefficient	$\alpha$	0.41	$\mu\text{m/m.K}$
Specific heat capacity	$C$	38	J/kg.K
Electrical resistivity	$R$	1.12	$\mu.\Omega.\text{m}$
Refractive index	$N$	5.48	-

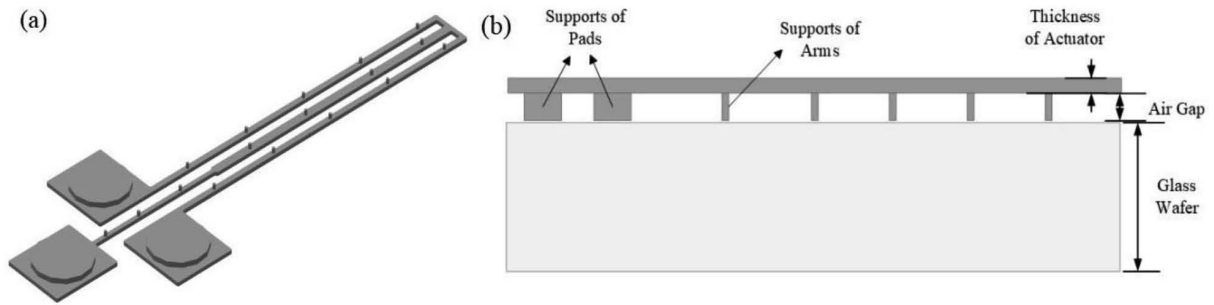


**Figure 6:** a) CAD design of the actuator. The structures at the top of the design were designed as the support; b) fabrication structure and design on the glass wafer

### 3 RESULTS AND DISCUSSION

#### 3.1 Fabrication with the 2PP technology

The bidirectional electrothermal microactuator, whose design is illustrated in **Figure 6a**, was fabricated utilizing a 2PP-technology-based Photonic Professional GT device.<sup>27</sup> There are supports to the arms and pads of this design. The number of supports to the arms is 17, the diameter is 2 μm and the height is 4 μm while the number of supports to the pads is 3, the diameter is 40 μm and the height is 4 μm. The dimensions of these supports are given in **Table 4**. Some unsuccessful experiments were done before this design. Fractures occurred during the fabrication when the number of supports to the arms was low. According to the experiments, the average distance between the supports should be 45 μm in order to avoid breakage. As the number of supports to the flexure arm is related to the cold arm, continuous

fractures occurred in experimental studies. A side view of the actuator on a glass wafer is given in **Figure 6b**. According to experimental studies, the maximum value of the resolution of a 3D printer should be 1 μm. Otherwise, the supports cannot be fabricated precisely. If the supports are not printed correctly, they cause collapses and breaks of the actuator.

**Table 4:** Dimensions of supports in the actuator

Parameter	Symbol	Value	Unit
Pad-support diameter	$r_{ps}$	40	μm
Arm-support diameter	$r_{as}$	2	μm
Support height	$h_s$	4	μm

An image of the actuator fabricated with the 2PP method is given in **Figure 7**. This image was taken with the microscope of the 3D printer.

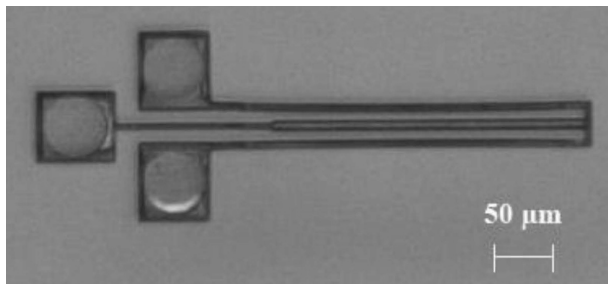


**Figure 7:** Image of the actuator fabricated with the 2PP method (photonic professional GT device’s camera)

#### 3.2 Fabrication with the PμSL technology

The bidirectional electrothermal microactuator, whose design is illustrated in **Figure 8a**, was fabricated using a PμSL-technology-based NanoArch™ series device.<sup>28</sup> The production of the supported design with this method was not possible for two reasons. First, the supported structures represent the system as a 3D design. However, it is not possible to produce 3D structures with the devices of the BMF Technology Company based on the PμSL technology. Second, these devices have a resolution of 2 μm and can fabricate a minimum thickness of up to 3 μm. When the support structures are removed, as

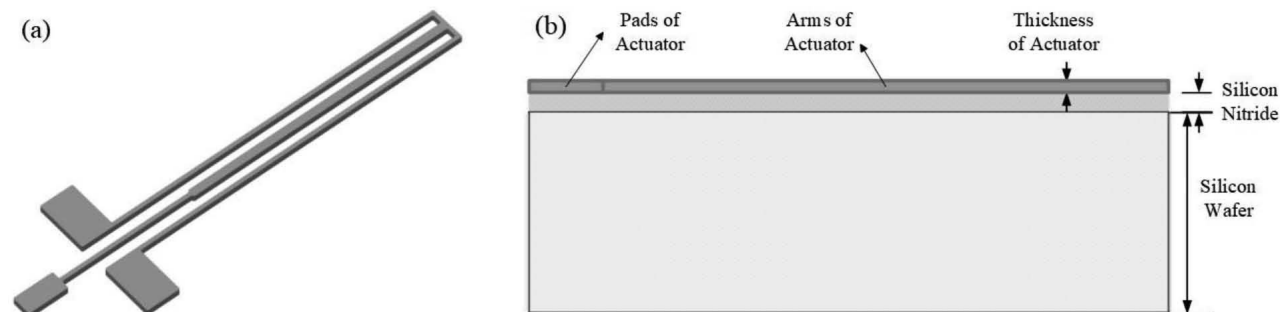


**Figure 8:** a) CAD design of the actuator. The support structures under the actuator are removed; b) for fabrication, the silicon wafer is coated with a sacrificial layer of silicon nitride



**Figure 9:** Image of the actuator fabricated with the P $\mu$ SL method (the NanoArch™ device's camera)

shown in **Figure 8a**, it is possible to perform the fabrication as the actuator design can be introduced to the device (a P $\mu$ SL-technology-based 3D printer) in two dimensions. The silicon wafer is coated with a sacrificial silicon nitride layer, used to separate the actuator from the silicon wafer, as shown in **Figure 8b**.

The image of the actuator produced with the P $\mu$ SL method is shown in **Figure 9**. This image was taken with the microscope of the 3D printer.

#### 4 CONCLUSIONS

In this study, a bidirectional electrothermal micro-actuator, fabricated with the traditional MEMS technique, was produced using the 2PP and P $\mu$ SL methods, which are 3D-printer procedures. These methods are the most common procedures used with 3D-printer devices.

When the experimental results were examined, it was observed that 2- $\mu$ m-diameter supports were produced with the 2PP method. However, it was not possible to produce them with the P $\mu$ SL method. The minimum structure that could be fabricated with the P $\mu$ SL method was 3  $\mu$ m in length. Structures smaller than 3  $\mu$ m could not be fabricated. Besides, the support structures could not be produced with the P $\mu$ SL method even when the diameters of the supports were 3  $\mu$ m. The support structures were then removed and a normal actuator production was performed. It was determined that the P $\mu$ SL method was not suitable for complex structures.

As a result of this study, it was found that the 2PP method is more appropriate since it allows the fabrication of more complex 3D structures with smaller dimensions, while the P $\mu$ SL method is only suitable for simple 2D micro-structures.

#### Acknowledgment

This study was supported by the Marmara University Scientific Research Projects Commission under project number FEN-C-DRP-101018-0536.

#### 5 REFERENCES

- <sup>1</sup> <https://www.nanoscribe.de/en/media-press/scientific-articles/>, 12.03.2019
- <sup>2</sup> Y. Li, Y. Fang, J. Wang, L. Wang, S. Tang, C. Jiang, L. Zheng, Y. Mei, Integrative optofluidic microcavity with tubular channels and

coupled waveguides via two-photon polymerization, *Lab on a Chip*, 16 (2016), 4406–4414, doi:10.1039/c6lc01148a

- <sup>3</sup> M. M. Sánchez, L. Schwarz, A. K. Meyer, F. Hebenstreit, O. G. Schmidt, Cellular cargo delivery: Toward assisted fertilization by sperm-carrying micromotors, *Nano Letters*, 16 (2015), 555–561, doi:10.1021/acs.nanolett.5b04221
- <sup>4</sup> C. Peters, M. Hoop, S. Pané, B. J. Nelson, C. Hierold, Degradable magnetic composites for minimally invasive interventions: Device fabrication, targeted drug delivery, and cytotoxicity tests, *Advanced Materials*, 28 (2016), 533–538, doi:10.1002/adma.201503112
- <sup>5</sup> L. C. Lay, M. R. Lee, H. K. Lee, I. Y. Phang, X. Y. Ling, Transformative two-dimensional array configurations by geometrical shape-shifting protein microstructures, *ACS Nano*, 9 (2015), 9708–9717, doi:10.1021/acsnano.5b04300
- <sup>6</sup> U. T. Sanli, H. Ceylan, I. Bykova, M. Weigand, M. Sitti, G. Schütz, K. Keskinbora, 3D nanoprinted plastic kinoform X-ray optics, *Advanced Materials*, 30 (2018), 12–21, doi:10.1002/adma.201802503
- <sup>7</sup> S. Thiele, K. Arzenbacher, T. Gissibl, H. Giessen, A. M. Herkommer, 3D-printed eagle eye: Compound microlens system for foveated imaging, *Science Advances*, 3 (2017), 124–131, doi:10.1126/sciadv.1602655
- <sup>8</sup> K. S. Worthington, L. A. Wiley, E. E. Kaalberg, M. M. Collins, R. F. Mullins, E. M. Stone, B. A. Tucker, Two-photon polymerization for production of human iPSC-derived retinal cell grafts, *Acta Biomaterialia*, 55 (2017), 385–395, doi:10.1016/j.actbio.2017.03.039
- <sup>9</sup> M. Suzuki, T. Tomokazu, A. Seiji, 3D laser lithographic fabrication of hollow microneedle mimicking mosquitos and its characterization, *International Journal of Nanotechnology*, 15 (2018), 157–173, doi:10.1504/IJNT.2018.089545
- <sup>10</sup> C. A. Lissandrello, W. F. Gillis, J. Shen, B. W. Pearre, F. Vitale, M. Pasquali, B. J. Holinski, D. J. Chew, A. E. White, T. J. Gardner, A micro-scale printable nanoclip for electrical stimulation and recording in small nerves, *Journal of Neural Engineering*, 14 (2017), 1056–1064, doi:10.1088/1741-2552/aa5a5b
- <sup>11</sup> R. Bogue, Energy harvesting: a review of recent developments, *Sensor Review*, 35 (2015), 1–5, doi:10.1108/SR-05-2014-652
- <sup>12</sup> C. Xia, L. Howon, F. Nicholas, Solvent-driven polymeric microbeam device, *Journal of Micromechanics and Microengineering*, 20 (2010), 19–24, doi:10.1088/0960-1317/20/8/085030
- <sup>13</sup> C. Xia, C. Andrew, Three-dimensional microfabricated bioreactors with the embedded capillary network, U.S. Patent Application No. 12/679,497
- <sup>14</sup> C. Sun, N. Fang, D. M. Wu, X. Zhang, Projection micro-stereolithography using digital micro-mirror dynamic mask, *Sensors and Actuators A: Physical*, 121 (2005), 113–120, doi:10.1016/j.sna.2004.12.011
- <sup>15</sup> J. Muskin, R. Matthew, G. Thomas, Three-dimensional printing using a photoinitiated polymer, *Journal of Chemical Education*, 87 (2010), 512–514, doi:10.1021/ed800170t
- <sup>16</sup> H. O. T. Ware, A. C. Farsheed, R. V. Lith, E. Baker, G. Ameer, C. Sun, Process development for high-resolution 3D-printing of bioresorbable vascular stents, *Advanced Fabrication Technologies for Micro/Nano Optics and Photonics X*, 5 (2017), 812–819, doi:10.1117/12.2252856
- <sup>17</sup> B. Lu, L. Hongbo, L. Hongzhong, Additive manufacturing frontier: 3D printing electronics, *Opto-Electronic Advances*, 1 (2018), 59–67, doi:10.29026/oea.2018.170004
- <sup>18</sup> J. K. Patel, C. Sun, H. F. Zhang, R. K. Talati, K. J. Patel, Compositions, systems and methods for the patient-specific ophthalmic device, U.S. Patent Application No. 15/543,490
- <sup>19</sup> J. H. Comtois, M. A. Michalick, C. C. Barron, Electrothermal actuators fabricated in four-level planarized surface micromachined polycrystalline silicon, *Sensors and Actuators A*, 70 (1998), 23–31, doi:10.1016/S0924-4247(98)00108-3
- <sup>20</sup> Q. A. Huang, N. K. S. Lee, Analysis and design of polysilicon thermal flexure actuator, *Journal of Micromechanics and Microengineering*, 9 (1999), 64–70, doi:S0960-1317(99)97876-2

- <sup>21</sup> K. S. Teh, Additive direct-write microfabrication for MEMS: A review, *Frontiers of Mechanical Engineering*, 12 (2017), 490–509, doi:10.1007/s11465-017-0484-4
- <sup>22</sup> S. Wu, J. Serbin, M. Gu, Two-photon polymerization for three-dimensional microfabrication, *Journal of Photochemistry and Photobiology A: Chemistry*, 181 (2006), 1–11, doi:10.1016/j.jphotochem.2006.03.004
- <sup>23</sup> X. Liu, H. Gu, M. Wang, X. Du, B. Gao, A. Elbaz, L. Sun, J. Liao, P. Xiao, Z. Gu, 3D printing of bioinspired liquid super repellent structures, *Advanced Materials*, 30 (2018), 375–381, doi:10.1002/adma.201800103
- <sup>24</sup> N.A. Bakhtina, U. Loeffelmann, N. MacKinnon, J. G. Korvink, Two-photon nanolithography enhances the performance of an ionic liquid–polymer composite sensor, *Advanced Functional Materials*, 25 (2015), 1683–1693, doi:10.1002/adfm.201404370
- <sup>25</sup> E. Baker, T. Reissman, F. Zhou, C. Wang, K. Lynch, C. Sun, Microstereolithography of three-dimensional polymeric springs for vibration energy harvesting, *Smart Materials Research*, 2012 (2012), 1–9, doi:10.1155/2012/741835
- <sup>26</sup> <http://bmftec.com/print/all>, 11.10.2018
- <sup>27</sup> S. Puce, E. Sciurti, F. Rizzi, B. Spagnolo, A. Qualtieri, M. Vittorio, U. Staufer, 3D-microfabrication by two-photon polymerization of an integrated sacrificial stencil mask, *Micro and Nano Engineering*, 2 (2019), 70–75, doi:10.1016/j.mne.2019.01.004
- <sup>28</sup> J. U. Surjadi, L. Gao, H. Du, X. Li, X. Xiong, N. X. Fang, Y. Lu, Mechanical metamaterials and their engineering applications, *Advanced Engineering Materials*, 21 (2019), 27–35, doi:10.1002/adem.201800864